Presented at CLAWAR 2004, in Madrid, Spain, Sept. 22-24, 2004

Towards Penetration-based Clawed Climbing

William R. Provancher[1], Jonathan E. Clark[1], Bill Geisler[2], and Mark R. Cutkosky[1]

[1] Department of Mechanical Engineering
Stanford University, Stanford, CA 94305 wil@cdr.stanford.edu
[2] Department of Biology
Lewis and Clark College, Portland, OR 97129

1 Introduction

Despite significant research focused on running robots, very little progress has been made towards legged robots that are capable of climbing in natural environments. Unlike their running counterparts, climbing robots must generate hand or foot holds capable of pulling them toward the substrate. The majority of efforts to develop climbing robots have been for urban settings with smooth glass or metal surfaces where suction and magnetic approaches to generating adhesion are possible. Some examples of robots that have used a suction based approach include [8, 10, 15]; some magnetic based climbers include [2, 13]. A few robots have also addressed climbing on rough rock surfaces, employing strong grips capable of sustaining tensile and shear loads [3, 4]. This paper describes efforts towards the development of a penetration-based clawed climbing robot capable of climbing on rough or smooth inclines.

1.1 Climbing in Natural Environments

Developing successful climbing robots for unstructured terrain or natural environments requires developing methods of generating adhesion, selecting a suitable sensor suite, developing locomotion strategies, and computing desired robot trajectories. In this paper, we focus on the first of these challenges.

As a starting point for selecting a mode of adhesion suitable for unstructured terrain, we look to the numerous examples found in nature. The primary modes of adhesion used by animals include wet and dry adhesion as well as claws or barbs. Some smaller animals, including Asian weaver ants, palmetto beetles, and tree frogs use wet-adhesion to stick to branches or trunks [6, 7]. However, the forces that can be generated from surface tension and capillary action in wet adhesion are not great enough to support large animals and may not be sufficient for small to medium scale robots.

Geckos, on the other hand, use dry-adhesion to stick to virtually any surface, no matter how slippery or shear. Geckos implement their van der Waals-based adhesion through millions of tiny hairs (setae) on their toes [1]. Recent experiments have shown that this mode of adhesion is capable of generating adhesive forces suitable for a small climbing robot [12]. The great potential and multitude of applications of this adhesive mechanism have motivated researchers to synthesize artificial dry adhesives [12]. However, practical artificial dry adhesives are not yet available.

Another approach to climbing, used by many larger mammals–including humans–utilizes cracks, ledges, and other types of hand holds to cling to a wall. Recently work has been done on developing robots [4] that use hand-hold and move like human rock climbers. These hand-hold based approaches, however, cannot be implemented in the absence of such surface irregularities. For a robot designed for rough terrain climbing, smooth impenetrable surfaces present the greatest challenge. On the other hand, a robot with claws designed to penetrate soft surfaces or engage an asperity on a rough surface does not need to rely on fortuitous hand or footholds to scale a wall. In fact, Mahendra [11] has shown that without claws even a gecko's ability to adhere to very rough surfaces is compromised.

1.2 Claw-based Climbing

For climbing on both rough and smooth penetrable surfaces, a claw-based approach is promising. Animals as small as insects and as large as bears use spines or claws when climbing. For example, cockroaches can climb an impressive range of materials by using their claws in conjunction with sticky metatarsal pads. However, in order to use claws effectively on a climbing robot, we need to develop engineering models of claw behavior, supported by empirical results.

Dai, et al. have used a simple model for clawed adhesion to predict frictional forces based on relative claw tip radius and surface roughness [5]. However, this model only considers shear forces generated when the insect foot interacts with a non-penetrable textured surface. For climbing it is also necessary to consider adhesive normal forces.

Many biologist have also investigated evolutionary adaptations specific to climbing. Zani [14] has looked specifically at lizard claws and toe morphology for climbing, showing improved clinging performance of shorter, stiffer claws on rough surfaces.

Recent research focused on observing cockroaches while climbing (unpublished experiments of D. Goldman and R. Full, UC-Berkeley) has shown that the roach's ability to climb shear surfaces is clearly effected by surface roughness. It appears that they rely on small irregularities in the substrate as footholds and therefore as surface roughness decreases, their ability to climb degrades.

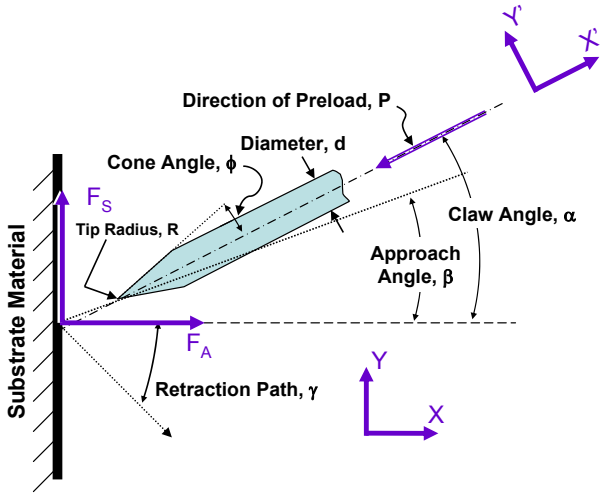

Fig. 1. Schematic showing test geometry, nomenclature, and conventions.

Consequently, for smooth, soft surfaces the best approach for a robotic climber may be to use claws to penetrate the substrate. To date, the primary work done on penetration and attachment to smooth surfaces comes from engineering, specifically the nail and staple industry [9].

Whether penetration or surface irregularities are utilized, a claw-based climbing robot has a number of challenges to overcome. Some of these include determining proper path generation, angle of attachment, and retraction angle. Other issues include dealing with ankle rotation during stance and keeping the claws sharp. This study takes the first step towards developing a viable claw-based climber by examining how claw tip geometry and insertion angle affect the ability of a claw to penetrate and grip a smooth penetrable surface.

2 Experimental Setup and Testing

To begin to answer these questions, we performed tests to determine how the geometry of claws affects their ability to penetrate a substrate and generate shear and adhesive forces. As shown in figure 1 we have designed a set of experiments to test the effect of varying claw diameter (d), cone angle (ϕ), and tip radius (R), as well as claw orientation (α), approach angle (β), and detachment angle (γ) relative to the substrate normal vector.

A first set of experiments were conducted with approach (β) and retraction (γ) angles fixed at 45° and −45°, respectively. A second set of experiments investigated the effect of varying the approach angle (β) on adhesive forces. In both sets of experiments, the claw angle (α) and the approach angle (β)

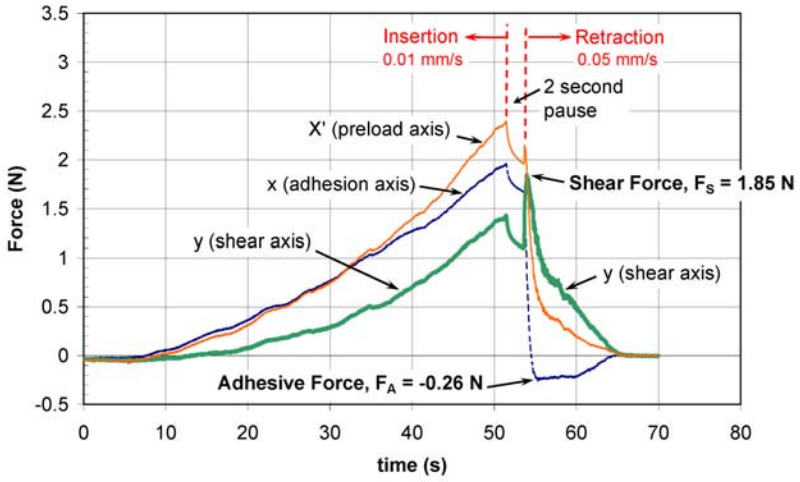

Fig. 2. A plot of a sample test run. This test was for a claw tip with diameter (d) of 1.5 mm, tip radius (R) of 30.5μm, and cone angle of 18°.

were identical. In both sets of experiments, the retraction angle, γ, of $-45°$ was chosen assuming that equal amounts of shear and adhesive forces would be required to scale a vertical wall.

Tests were performed using a Newport ESP-300 motion controller driving 850G and 850G/HS actuators on a 461XYZLM stage. In all tests, the barbs were inserted and retracted at a constant rate of 0.01 mm/s and 0.05 mm/s. Approximate preloads were prescribed by programming insertion displacement appropriately. Forces were measured in the X' and Y' axes (see figure 1) using a Kistler 9328A piezoelectric 3-axis force sensor and 5010B charge amplifiers. Drift in these force sensors was corrected in post-processing of data by assuming a constant drift rate and adjusting each force channel by a proportional offset, based on the no-load force readings at the end of each set of trials. Data were acquired with MacLab A/D converter on an Apple Powerbook G3 at 40 Hz.

2.1 Experimental Results

A typical claw adhesion test is shown in figure 2 (for barb no. 8). In each test the claw tip was driven into the substrate (soft wood) a finite displacement along the approach angle (β) and then, following a 2 second pause, was forcibly removed along the retraction path (γ). This test shows a peak preload of 2.2 N on the X'-axis, and a maximum adhesive force of -0.26 N. The claw also generated a 1.85 N plowing (shear) force.

As shown in Table 1, barb geometry in the first set of experiments covered the following range: wire diameter, $d = 0.51$ to 1.50 mm diameter, cone angle,

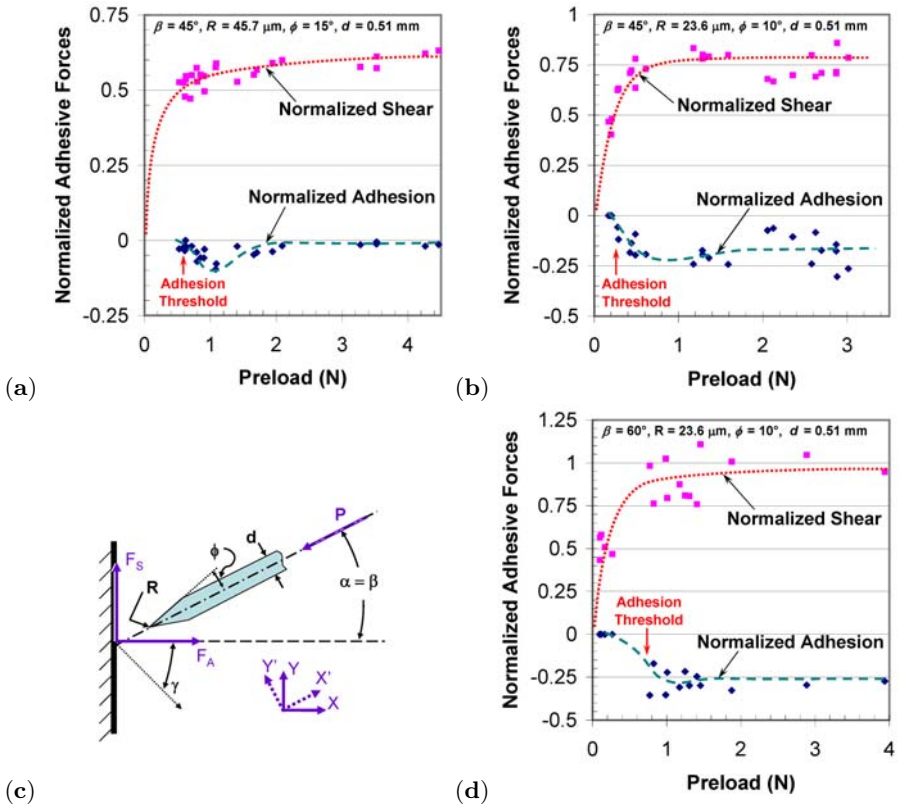

Fig. 3. A plot of results for $d = 0.51$ mm barbs. Shear and adhesion values are normalized by dividing by the applied preload, designated (F_S/P) and adhesion (F_A/P), respectively. Normalized adhesive forces are shown for (**a**) experiment 1, barb 1, (**b**) experiment 1, barb 2, and (**d**) experiment 2, barb 2, respectively. A simplified version of figure 1 is shown in (c) for reference.

$\phi = 10$ to 21°, and tip radius, $R = 15.7$ to 121.9 μm. Data were collected in 25 trials for each barb with preloads ranging from 0.095 to 9.38 N (barb no. 8 was only tested in 21 trials). To make it easier to compare adhesive forces (on adhesion, x, and shear, y, axes) generated for various preloads, they are normalized by dividing adhesive forces by the preload for each respective trial. The average of normalized adhesive values for each set of trials is reported in Table 1 along with the standard deviation. Observe that in each case where two barbs of the same diameter, but with different tip radius, R (e.g., barbs 1 and 2), that the one with the smaller tip radius performs better. In addition, those with smaller tip radius also have a lower threshold for adhesion, as shown in a comparison of figures 3(a) and (b).

Table 1. Results of first experiment, investigating effect of varying barb diameter (d), cone angle (ϕ), and tip radius (R). The mean of normalized shear and adhesion forces are reported, designated $\overline{(F_S/P)}$ and $\overline{(F_A/P)}$, respectively. The data were normalized by dividing by the applied preload for each respective trial. Mean values are listed with ± one standard deviation.

barb no.	d (mm)	ϕ (°)	R (μm)	$\overline{(F_A/P)}$	$\overline{(F_S/P)}$
1	0.51	15	45.7	0.029 ± 0.029	0.555 ± 0.041
2	0.51	10	23.6	0.146 ± 0.085	0.700 ± 0.113
3	0.79	14	25.4	0.154 ± 0.038	0.873 ± 0.072
4	0.99	10	15.7	0.149 ± 0.050	0.746 ± 0.044
5	1.24	15	88.9	0.046 ± 0.051	0.558 ± 0.060
6	1.24	21	27.9	0.105 ± 0.045	0.733 ± 0.065
7	1.50	14	121.9	0.057 ± 0.061	0.598 ± 0.095
8	1.50	18	30.5	0.092 ± 0.068	0.662 ± 0.134

Table 2. Results of second experiment, investigating effect of varying the approach angle (β). These tests were conducted with the second barb from experiment 1 (d = 0.51mm, $\phi = 10°$, and $R = 23.6$ μm). As in Table 1, the mean of normalized shear and adhesion forces are reported, designated $\overline{(F_S/P)}$ and $\overline{(F_A/P)}$, respectively.

β (°)	$\overline{(F_A/P)}$	$\overline{(F_S/P)}$
15	0.0393 ± 0.0437	0.2557 ± 0.1021
30	0.1092 ± 0.0771	0.5224 ± 0.1611
45	0.2328 ± 0.1570	0.6683 ± 0.1423
60	0.1981 ± 0.1399	0.7928 ± 0.2158

Results for $\beta = 75°$ experiments omitted – barb did not penetrate.

After establishing a good tip geometry, the goal of second experiment was to investigate what approach angle, β, is optimal for generating adhesive forces. Tests were completed for β = 15, 30, 45, 60, and 75°. 25 trials were completed for each approach angle (17 were completed for $\beta = 60°$). No trials were completed successfully for $\beta = 75°$, because the barb never penetrated the wood. Barb 2 was chosen for these experiments because of its relatively good performance in experiment 1. Results for the second set of experiments are reported in Table 2. Barbs tested at $\beta = 45°$ have the highest adhesion, while more shear force was produced at $\beta = 60°$. A comparison of figures 3(b) and (c) shows that $\beta = 45°$ has the lowest preload threshold for adhesion. No wear (dulling) was observed for either sets of experiments.

3 Discussion and Application to Climbing Robots

Preliminary experiments show that tip radius (R) far outweighs the influence of cone angle (ϕ) on measured shear and normal adhesion forces. We also

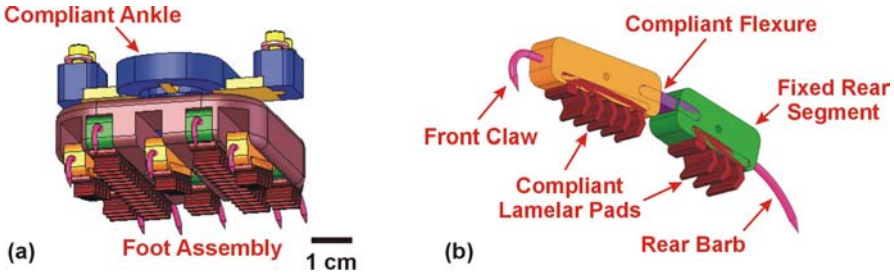

Fig. 4. A preliminary CAD model concept of a proposed robot (**a**) foot and (**b**) toe. A number of toe assemblies would be combined to form a foot.

found that shear and adhesion forces were roughly proportional to preload. For example, with the sharpest claws, we found that we could generate shear forces of up to 103% of the applied preload, and adhesive forces up to 34% of the preload. This percentage, however, decreased as the preload increased if claws were not sharp (as seen in figure 3(a)). In fact, decreasing adhesion at higher preloads is also the primary cause of the high adhesion standard deviations reported for barb numbers 1, 5, and 7 in Table 1. Since barbs will tend to dull with wear, this suggests that distributing the preload over many independently sprung claws may be advantageous. We also observe that adhesion is more greatly affected by barb tip geometry than shear. The second experiment suggests that an approach angle and barb orientation of 45 to 60° is desirable for generating optimal adhesion.

These observations guided the design of our initial prototype foot. A CAD model of a climbing foot and individual toe from this prototype is shown in figure 4. Our prototype includes multiple claws and compliance as inspired by these findings and the cockroach foot design. Future prototypes will have multiple toes per foot and multiple pins per toe. Compliance on each toe will allow a maximum number of toes to engage on rough terrain.

The design in figure 4 has the nominal claw angle of $\alpha = 60°$ that rotates to 45° when the foot contacts the surface and compresses the toes. This design works relatively well, however, the data suggests that the claws should actually rotate the opposite direction when they contact the surface. Setting the nominal claw angle to $\alpha = 45°$ would allow the lowest possible preload threshold for adhesion. Once initial claw engagement has transpired, rotating the claw toward 60° will allow the maximum adhesion. A toe design as shown in figure 5, though slightly more complex than the initial prototype would accomplish this goal. This design could be purely passive, as suggested by the schematic 4-bar linkage shown in figure 5, with an instantaneous center of rotation at the wall surface. Note that in addition to the preferential barb orientation, this type of toe design also pulls in towards the surface as shearing load from the weight of the robot is applied to the claws.

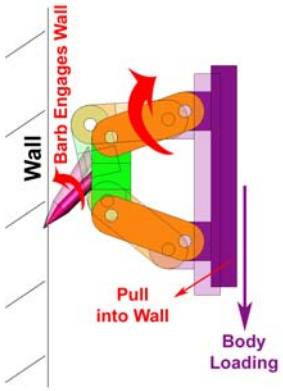

Fig. 5. Kinematic concept of passively engaging claw. The mass of the robot induces rotation of the linkage after initial attachment to the climbing substrate.

4 Conclusions

Our results show that claws are promising for smooth surfaces. Our experiments show a preferred claw geometry (small tip radius, R) and insertion angles, $\beta = 45 - 60°$, for good adhesion and shear. The experiments also suggest having many claws to distribute the required adhesive forces and reduce loading on each claw. To accomplish this, claws will need to be independently sprung, necessitating more complex foot designs and raising the bar for meso-scale manufacturing.

This first set of experiments has just scratched the surface of this challenging problem. To better understand the sensitivity of claw orientation on foot attachment, future experiments will look at varying claw orientation and approach angles independently as well as varying retraction angles. We will also focus on the range between 45 and 60° for the optimum barb orientation. Once these effects are better understood, testing at higher impact velocities and testing at the toe level will ensue, to determine how to design toe compliance. For materials other than soft wood, the strain rate is may be important so that quasi-static tests as reported here will no longer suffice. In the future we will investigate simple models of claw penetration and adhesion and their correlation with experiments.

Acknowledgements

This work was supported by the DCI Postdoctoral Fellow Program under grant number MNA501-03-12002 and by DARPA under grant number NC66001-03-C-8045. The authors also thank Kellar Autumn from Lewis and Clark College for access to lab facilities used to run these experiments.

References

1. K. Autumn and A. Peattie. Mechanisms of adhesion in geckos. *Integrative and Comparative Biology*, 42(6):1081–1090, 2002.
2. C. Balaguer, A. Gimenez, J.M. Pastor, V.M. Padron, and C. Abderrahim. A climbing autonomous robot for inspection applications in 3d complex environments. *Robotica*, 18:287–297, 2000.
3. D. Bevly, S. Dubowsky, and C. Mavroidis. A simplified cartesian-computed torque controller for highly geared systems and its application to an experimental climbing robot. *Transactions of the ASME. Journal of Dynamic Systems, Measurement and Control*, 122(1):27–32, 2000.
4. T. Bretl, S. Rock, and J.C. Latombe. Motion planning for a three-limbed climbing robot in vertical natural terrain. In *Proceedings of the IEEE International Conference on Robotics and Automation*. Piscataway, NJ, USA : IEEE, 2003.
5. Z.D. Dai, S.N. Gorb, and U. Schwarz. Roughness-dependent friction force of the tarsal claw system in the beetle pachnoda marginata (coleoptera, scarabaeidae). *Journal Of Experimental Biology*, 205(16):2479–2488, 2002.
6. S.B. Emerson and D. Diehl. Toe pad morphology and mechanisms of sticking in frogs. *Biological Journal of the Linnean Society*, 13(3):199–216, 1980.
7. W. Federle, M. Riehle, A.S.G. Curtis, and R.J. Full. An integrative study of insect adhesion: mechanics and wet adhesion of pretarsal pads in ants. *Integrative and Comparative Biology*, 42(6):1100–1106, 2002.
8. G. La Rosa, M. Messina, G. Muscato, and R. Sinatra. A low-cost lightweight climbing robot for the inspection of vertical surfaces. *Mechatronics*, 12(1):71–96, 2002.
9. Forest Products Laboratory. Nail-withdrawal resistance of american woods. *U. S. Department of Agriculture - Forest Service*, 1965.
10. R. Lal Tummala, R. Mukherjee, N. Xi, D. Aslam, H. Dulimarta, Jizhong Xiao, M. Minor, and G. Dang. Climbing the walls [robots]. *IEEE Robotics and Automation Magazine*, 9(4):10–19, 2002.
11. B.C. Mahendra. Contributions to the bionomics, anatomy, reproduction and development of the indian house gecko hemidactylus flaviviridis ruppell. part ii, the problem of locomotion. volume 13, pages 288–306. Proc. Indian Acad. Sci., Sec. B, 2003.
12. M. Sitti and R.S. Fearing. Synthetic gecko foot-hair micro/nano-structures for future wall-climbing robots. In *Proceedings of the IEEE International Conference on Robotics and Automation*, volume 1, pages 1164 – 1170. Piscataway, NJ, USA : IEEE, 2003.
13. Z.L. Xu and P.S. Ma. A wall-climbing robot for labelling scale of oil tank's volume. *Robotica*, 20:209–212, 2002.
14. P.A. Zani. The comparative evolution of lizard claw and toe morphology and clinging performance. *Journal of Evolutionary Biology*, 13:316–325, 2000.
15. J. Zhu, D. Sun, and S.K. Tso. Development of a tracked climbing robot. *Journal Of Intelligent And Robotic Systems*, 35(4):427–444, 2002.